NANOSYSTEMS:
PHYSICS, CHEMISTRY, MATHEMATICS

Original article

Fedorov P.P., Novikov I.A., et al. *Nanosystems: Phys. Chem. Math.*, 2022, **13** (5), 539–545.
http://nanojournal.ifmo.ru
DOI 10.17586/2220-8054-2022-13-5-539-545

Transformation of siderite in the zone of hypergenesis

Pavel P. Fedorov[a], Ivan A. Novikov[b], Valery V. Voronov[c], Lubov V. Badyanova[d], Sergey V. Kuznetsov[e], Elena V. Chernova[f]

Prokhorov General Physics Institute of the Russian Academy of Sciences, Moscow, 119991, Russia

[a]ppfedorov@yandex.ru, [b]ivan.a.novikov@gmail.com, [c]voronov@lst.gpi.ru, [d]badyanova.lubov@gmail.com, [e]kouznetzovsv@gmail.com, [f]e-chernova@yandex.ru

Corresponding author: Pavel P. Fedorov, ppfedorov@yandex.ru

ABSTRACT The structure of siderite aggregates and its weathering products from the Ruza deposit, Moscow Region, has been studied by X-ray phase analysis and electron microscopy. The initial siderite is a dense $FeCO_3$ aggregate of micron-sized grains. The nodules are covered with an ocher weathered crust, the color intensity of which varies from light yellow to brown-black. A successive replacement of siderite by FeOOH goethite and lepidocrocite was revealed. It is accompanied by a sharp decrease in volume ($\sim$ 30 %) and the formation of a microporous structure.

KEYWORDS carbonates, siderite, weathering, oxidation, nanomineralogy

ACKNOWLEDGEMENTS The equipment of the Collective Use Centers of the GPI RAS and IGEM RAS was used in this work.

FOR CITATION Fedorov P.P., Novikov I.A., Voronov V.V., Badyanova L.V., Kuznetsov S.V., Chernova E.V. Transformation of siderite in the zone of hypergenesis. *Nanosystems: Phys. Chem. Math.*, 2022, **13** (5), 539–545.

1. Introduction

Siderite (a ferrous II carbonate $FeCO_3$) is a widespread mineral [1–4]. It is isostructural to calcite, crystallizes in hexagonal crystal system, SSG *R*-3*m*. In spite of its widespread occurrence, siderite is of limited use as a crude for ferrous metallurgy. The products of natural alteration of siderite in the hypergenesis zone, known as *iron hat*, or limonite, has a greater practical importance. The common popular name "bog ore" is very unfortunate, because the genesis of these formations, as a rule, has nothing to do with swamps. Many siderite deposits are of industrial importance, in particular, the Bakal deposit (the South Urals, the Chelyabinsk region) [5–10]. But the direct use of siderite ore from this and similar deposits is impossible. The preparation of raw materials for the subsequent steelmaking includes the obligatory energy-consuming process of annealing in an oxidizing flame, which only partially repeats the weathering process.

The purpose of this work is a study of the siderite transformation mechanism in zone of hypergenesis, i.e. in the process of weathering.

2. Experimental section

2.1. Materials

Among many samples of siderite of sedimentary origin, we chose one with a small amount of chemical and mechanical impurities. The sample was taken from a small deposit of siderite, which is exposed near Ruza (Moscow Region) [11]. A distinctive feature of this deposit is low content of magnesium in siderite. According to rough estimates, about 30 000 tons of ore were excavated and used for metallurgical production in the Middle Ages. Partially limonitized siderite forms lenses in the upper part of the Carboniferous limestones. Siderite forms solid masses of a grayish-greenish color and is covered with yellow-brown crusts of iron hydroxides (Fig. 1). We will call the totality of iron hydroxides, mechanical impurities and associated minerals "limonite", despite the fact that this is not a strict mineralogical term. Associated minerals are calcite $CaCO_3$, nickel-bearing rancieite $(Ca, Mn^{2+}, Ni^{2+})_{0.2}(Mn^{4+}, Mn^{3+})O_2 \cdot 0.6H_2O$, and natrojarosite $NaFe_3^{3+}(SO_4)_2(OH)_6$.

FIG. 1. General view of the sample: central zone – siderite (*), outer zones - cocentric aggregate of limonite (natural oxidation products)

2.2. Characterization

X-ray diffraction analysis (XRD) of the samples was carried out on a BRUKER D8 ADVANCE diffractometer with CuKα_1 radiation. The lattice parameters and sizes of domains of coherent scattering (D) were calculated using the TOPAS software Version 4.2.0.2 ($R_{wp} < 5$).

The determination of the concentration of major oxides and some trace elements in natural samples was performed by X-ray fluorescence analysis (XRF) on a sequential vacuum spectrometer (with wavelength dispersion), AxiosmAX model by PANalytical (Netherlands) (www.panalytical.com). The spectrometer is equipped with 4 kW X-ray tube with Rh anode. Maximum tube voltage 60 kV, maximum anode current 160 mA.

The preparations were made from sample powder by melting with a mixture of lithium borates at a temperature of 1150 °C to analyze of rock-forming oxides. From the resulting borate melt, glassy disks were formed, which were analyzed in the spectrometer. To determine trace elements, sulfur and chlorine, preparations were made from sample powder by cold pressing with plastic filler under a pressure of 30 tons into tablets with diameter of 32 mm, which were analyzed in the spectrometer.

The weight loss on calcination (WL) was measured from samples dried at 110 °C according to the NSAM VIMS 118-X method at a temperature of 1000 °C.

For visualization, we used a scanning electron microscope EVO LS10 (Zeiss, Germany) with LaB_6 cathode. The observations were performed with accelerating voltage of 21 kV with backscattered (reflected) electron detector (BSE). Microstructure of specimen was visualized in the low vacuum mode (EP, 70 Pa) with the working distance of 6.5 – 4.5 mm.

Thermogravimetry analysis was made with a Q-1500 D derivatograph in platinum crucibles at the sample weight of 300 mg and the rate of heating under air of 10 °C/min.

3. Results and discussion

According to chemical analysis, the original siderite and its oxidation products have a similar set of main impurities (Table 1). For the main components, a significant decrease in the content of calcium and an increase in the content of iron and silicon in natural limonite can be noted in relation to the original substrate. The behavior of impurities is different. The magnesium content decreases when the transition of siderite to limonite takes place, while sodium and sulfur content increases. Phosphorus and manganese remain unchanged. The evolution of the chemical composition during the natural oxidation of siderite looks logical. Since the active agent during weathering is water, the depletion of the initial substrate in alkaline earth elements is natural. The increase in the content of sodium and sulfur in the oxidation products is probably due to the admixture of natrojarosite. The formation of natrojarosite at this deposit occurred during the later modifications of the mineral substance is not associated with the weathering process and is not considered in this study.

The results of the X-ray study are shown in Fig. 2, electron microscopy data are shown in Fig. 3. As it is seen from the SEM data, the original mineral consists of $FeCO_3$ grains 5 – 10 μm in size. The size of the regions of coherent reflection scattering with the Miller index (104) was $D = 26$ nm.

According to XRD data, white edging at the boundary of the weathering zone contains, along with the main mass of siderite, an initial amount of goethite. The yellow (light ocher) zone contains mostly goethite with some siderite. The dark brown zone is mainly composed of goethite. There is also a small amount of lepidocrocite (Fig. 2). The size of the coherent scattering regions for the goethite phase in reflection (110) was $D = 14 – 18$ nm.

TABLE 1. Chemical composition of siderite and limonite

	WL 1000 °C (%)	WL	(wt %)											
			Na_2O	MgO	Al_2O_3	SiO_2	K_2O	CaO	TiO_2	MnO	FeO (total)	P_2O_5	Cl	SO_3 (total)
Siderite	31.61	(CO_2)	0.05	0.67	1.22	2.96	0.09	2.83	0.02	0.58	59.46	0.138	0.01	0.03
SD	0.36		0.01	0.09	0.13	0.20	0.02	0.19	0.01	0.08	0.48	0.029	0.01	0.01
Limonite	14.36	(H_2O)	0.33	0.34	1.41	4.85	0.07	0.76	<0.01	0.67	76.61	0.163	0.05	0.11
SD	0.31		0.05	0.05	0.16	0.33	0.02	0.09	—	0.09	0.54	0.034	0.02	0.01

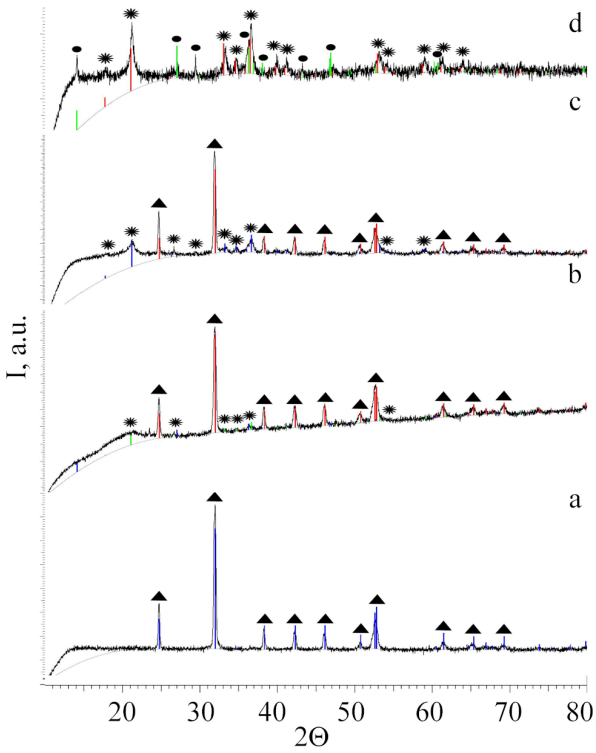

FIG. 2. X-ray diffraction patterns of siderite and weathering crust samples: a – central part ($D_{\text{siderite}} = 26$ nm), b – bleaching zone ($D_{\text{siderite}} = 23$ nm), c – light ocher zone ($D_{\text{siderite}} = 28$ nm, $D_{\text{hetite}} = 14$ nm), d – dark brown zone ($D_{\text{hetite}} = 18$ nm). Triangles – siderite $FeCO_3$, asterisks – goethite FeOOH, dots – lepidocrocite FeOOH

Based on the initial and final products, the weathering reaction can be written as follows:

$$4FeCO_3 + 2H_2O + O_2 \longrightarrow 4FeOOH + 4CO_2 \uparrow . \quad (1)$$

Goethite and lepidocrocite have the same chemical composition: FeOOH. Thus, in accordance with equation (1), weathering of siderite is not a pure oxidation process: in addition to oxygen, which provides an increase in the valence of iron from $+2$ to $+3$, the reaction also requires the participation of water. At the first stage of the reaction, water and oxygen, apparently, penetrate into the siderite mass along the grain boundaries.

It should be noted that reaction (1) is accompanied by a very sharp decrease in volume. Molar volume of goethite is as follows $V = 138.60$ Å^3 (JCPDS card #29-713), $Z = 4$, $V/Z = 34.65$ Å^3, for siderite: $V = 293.53$ Å^3 (JCPDS card #73-6522), $Z = 6$, $V/Z = 48.86$ Å^3.

Thus, the shrinkage is 29 %. Note that in the remarkable work of Zemyatchensky [12], performed in the pre-X-ray period, the shrinkage value of 31 % was calculated based on the experimental values of the density of minerals. Reaction (1), once started, leads to the appearance of shrinkage cavities and microcracks, which facilitates the delivery of oxygen and the removal of the reaction product CO_2 from the front of the chemical reaction and ensures its further flow.

Electron microscopy reveals the details of this process (Fig. 3). In the process of weathering, the contours of the initial grains, originally formed by siderite, practically do not change, which can be seen from a comparison of

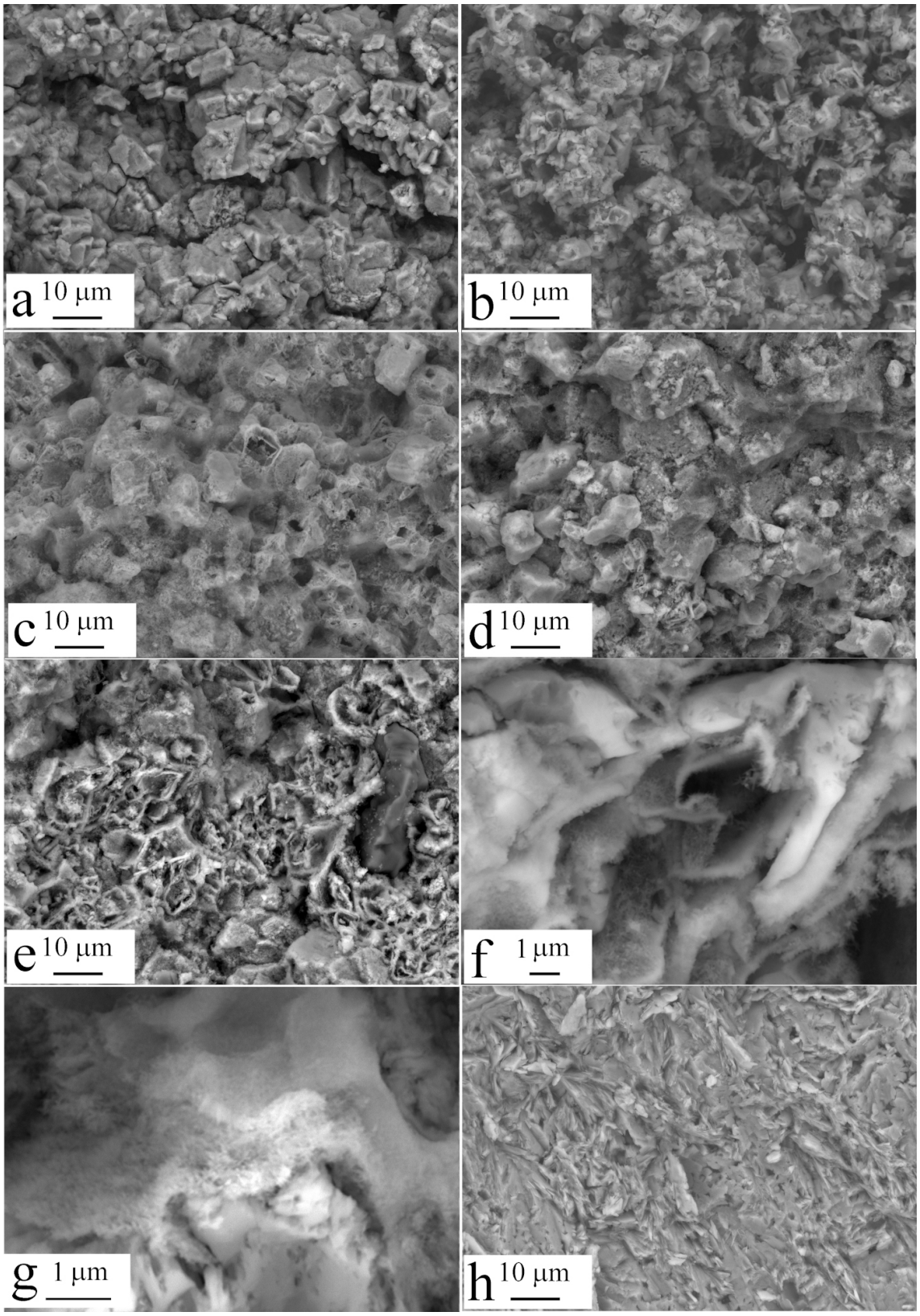

FIG. 3. Micrographs of siderite samples and weathering products. a – original siderite, b – bleaching zone, c – light ocher zone, d, e, f, g – brown zone, h – dark brown zone (goethite-lepidocrocite aggregate)

Figs. 3(a–d). However, this is only a visual resemblance. Siderite grains are replaced by a porous (spongy) aggregate of iron hydroxides.

Details of the formation of porous aggregate can be seen at the microscale (Figs. 3(e–g)). The resulting goethite particles shrink into two-dimensional films. At the beginning of the process, these films follow the contour of the original siderite grain. Further corrosion of siderite occurs with a decrease in the size of its single crystals and with their partial fragmentation *in situ* along cleavage planes (Fig. 3(f)). Periodically formed two-dimensional films of goethite repeat the shape of the surface of continuously decreasing siderite crystals and their fragments. The nature of the periodicity is not entirely clear. During the reaction, the surface of the initial grain recedes, but until a certain moment the cavity is filled with reaction products, and the resulting film of goethite nanocrystals adjoins siderite. Then the agglomerate of the reaction products and the original crystal are separated. For some time, the two-dimensional film continues to accept the reaction products and thicken without contact with the receding surface of the siderite crystal. The gap between them increases to 0.1 – 0.4 mm, which is probably the threshold value that partially determines the nature of the periodicity of the process at the nanoscale. Upon reaching this value, a new reaction layer is nucleated directly on the surface of the reduced siderite microcrystal, and the process is repeated.

At the microscale, this process leads to formation of a box-like (shell-shaped) structure with microcavities, open for access and removal of reagents (Figs. 3(f,g)). The proportion of free volume in these grains is about 30 % according to calculations.

According to XRD data, the size of the coherent scattering regions D of siderite practically does not change (Fig. 2).

Thus, reaction (1) describes a system with positive feedback. Such systems are characterized by nonlinear dynamics, which leads to periodic reaction.

The same periodicity is observed at the macroscale. The structure of the aggregate shows alternation of yellow and brown concentric zones in the crust around the core of initial siderite, similar to Liesegang rings [13, 14] (Fig. 1). The yellow and brown zones correspond to different degrees of goethite filling of the cavities in the spongy aggregate. Within the brown zones, the primary microscopic picture of the porous siderite oxidation product changes due to the filling of microscopic cavities with newly formed goethite and recrystallization (Fig. 3(h)). Despite this, the general appearance of the concentric-zonal aggregate fully confirms the deficient nature of the reaction in terms of volume. Cavities can be seen between the zones, and contraction cracks across the layers. The completed weathering process leads to the formation of hollow geodes, which are often found in the deposit.

As we have shown, at the micro level, the newly formed goethite aggregate repeats the contours of siderite grains, and at the macro level, the limonite zones repeat the primary contours of the siderite ore block. This situation can be described in terms of pseudomorphosis [15, 16], but not in terms of topotaxy [17, 18]: topotaxy in the narrow sense of the word implies an oriented growth of solid reaction products on the initial substrate.

There is a noticeable analogy of the discussed reaction with the process of interaction of calcium carbonate with a solution of potassium fluoride, in which the volume of fluorite nanoparticles formed is about 2/3 of the initial volume of calcium carbonate micrograins [19, 20].

It is the microporosity of the weathering products of siderite that ensures their successful use in ferrous metallurgy as iron ore [12]. Although it is energetically much more profitable to restore metallic iron from compounds in the $+2$ oxidation state than $+3$, kinetic difficulties make it impossible to use $FeCO_3$ in this capacity, because the density of siderite aggregates blocks the penetration of the reducing agent – carbon monoxide – into the volume. Weathering products differ radically from the original material in this respect.

The process of change in the hypergenesis zone differs significantly from the process of artificial oxidation of siderite ores, carried out in the preparation of the charge for the blast-furnace and converter processes [8–10].

The results of DTA heating a siderite sample under air are shown in Fig. 4. Weight loss starts at 385 °C and ends at 539 °C. The process has a two-stage character. According to XRD data (Fig. 5), the final product is hematite Fe_2O_3 with a small admixture of magnetite Fe_3O_4. The sequence of oxidation can be described by the following reactions:

$$FeCO_3 \longrightarrow FeO + CO_2 \uparrow, \tag{2}$$

$$3FeO + 1/2O_2 \longrightarrow Fe_3O_4, \tag{3}$$

$$2Fe_3O_4 + 1/2O_2 \longrightarrow 3Fe_2O_3. \tag{4}$$

4. Conclusion

Transformation of siderite in the zone of hypergenesis (weathering reaction) is not oxidation in its pure form, because it includes the mandatory participation of water. The transformation of minerals in this case does not occur through dissolution followed by precipitation [5]. We also did not record the formation of an amorphous phase in the weathering crust [3]. The process occurs with the preservation of the shape and volume of the original siderite grains. However, due to a sharp decrease in volume during the transformation of siderite into goethite, a microporous structure is formed. The weathering process of siderite belongs to the field of nanomineralogy.

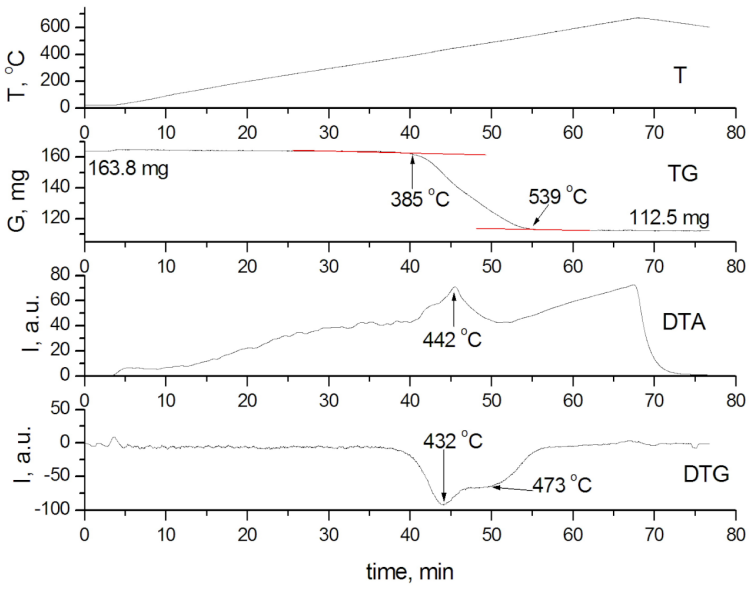

FIG. 4. Derivatogram of a siderite sample

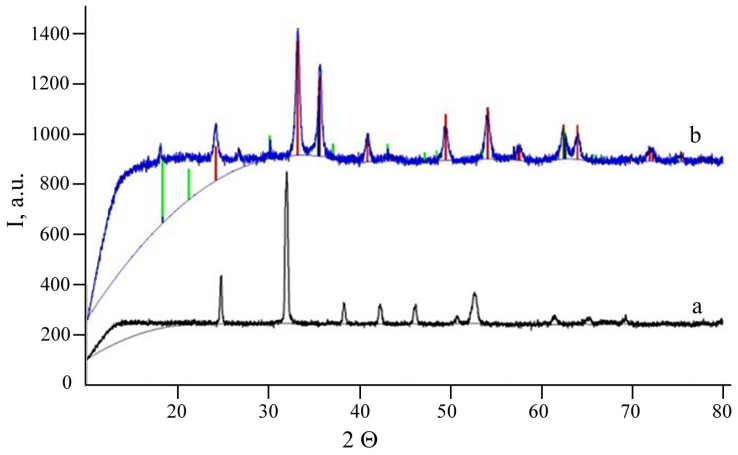

FIG. 5. XRD of the original sample (a) and the sample after thermogravimetry (b)

References

[1] Godovikov A.A. *Mineralogy*. M.: Nedra, 1983 (in Russian).
[2] Kholodov V.N., Butuzova G.Yu. Problems of Siderite Formation and Iron Ore Epochs: Communication 2. General Issues of the Precambrian and Phanerozoic Ore Accumulation. *Lithology and Mineral Resources*, 2004, **39** (6), P. 489–508.
[3] Kholodov V.N., Butuzova G.Yu. Siderite Formation and Evolution of Sedimentary Iron Ore Deposition in the Earth's History. *Geology of Ore Deposits*, 2008, **50** (4), P. 299–319.
[4] Liao Shipan, Liang Tongrong, Zeng Mingguo. Geochemical Characteristics of Gossans Related to Siderite Deposits in Carbonate Strata, Western Guizhou. *Geochemistry*, 1983, **2** (4), P. 279–292.
[5] Yanitskii Ya.L., Sergeev O.P. *Bakal iron ore deposits and their genesis*. M.: USSR Acad. Sci., 1962 (in Russian).
[6] Timeskov V.A. *Mineralogy of carbonate ores and host carbonate rocks of the Bakal iron ore deposit in the South Urals*. Kazan': Kazan' University, 1963 (in Russian).
[7] Ellmies R., Voigtländer G., et al. Origin of giant stratabound deposits of magnesite and siderite in Riphean carbonate rocks of the Bashkir mega-anticline, western Urals. *Geologische Rundschau*, 1999, **87** (4), P. 589–602.
[8] Klochkovskii S.P., Smirnov A.N., Savchenko I.A. Development of physical and chemical bases for the integrated use of high-magnesian siderites. *Vestnik G.I. Nosov MGTU*, 2015, **1**, P. 26–31 (in Russian).
[9] Matyukhin V.I, Melamud S.G., et al. The investigation of firing of siderite small fractions in a rotary furnace. *Izvestiya. Ferrous Metallurgy*, 2015, **58** (9), P. 652–657 (in Russian).
[10] Sheshukov O.Yu., Mikheenkov M.A., et al. Changes in phase composition of siderites of the bakal deposit at heating. *Izvestiya. Ferrous Metallurgy*, 2018, **61** (11), P. 891–897 (in Russian).
[11] URL: https://webmineral.ru/minerals/image.php?id=5030
[12] Zemyatchenskii P. Iron ores of the central part of European Russia. *Proceedings of the Society of Naturalists*, St.-Petersburg, 1889, **20**.
[13] Shemyakin F.M., Mikhalev P.F. *Physico-chemical periodic processes*. L.: USSR Acad. Sci.,, 1938. (in Russian)
[14] Summ B.D., Ivanova N.I. The use of objects and methods of colloid chemistry in nanochemistry. *Russian Chemical Rev.*, 2000, **69**, P. 911.

[15] Glover E.D., Sippel R.F. Experimental pseudomorphs: replacement of calcite by fluorite. *American Mineralogist*, 1962, **47**, P. 1156–1165.
[16] Glikin A.E. *Polymineral metosomatic crystallogenesis*. St.-Petersburg: Neva, 2004 (in Russian).
[17] Shannon R., Rossi R. Definition of Topotaxy. *Nature*, 1964, **202**, P. 1000–1001.
[18] Oleinikov N.N. Effect of topochemical memory: nature and role in the synthesis of solid-phase substances and materials. *Rus. Chim. J.*, 1995, **39**, P. 85–93.
[19] Fedorov P.P., Luginina A.A., Alexandrov A.A., Chernova E.V. Transformation of calcite $CaCO_3$ to fluorite CaF_2 by action of KF solution. *J. Fluorine Chemistry*, 2021. **251**, 109898.
[20] Fedorov P.P., Luginina A.A., et al. Interaction of calcium and strontium carbonates with KF solution. *Russ. J. Inorg. Chem.*, 2022, **8**.

Submitted 3 July 2022; revised 15 September 2022; accepted 19 September 2022

Information about the authors:

Pavel P. Fedorov – Prokhorov General Physics Institute of the Russian Academy of Sciences, Moscow, 119991, Russia; ORCID 0000-0002-2918-3926; ppfedorov@yandex.ru

Ivan A. Novikov – Prokhorov General Physics Institute of the Russian Academy of Sciences, Moscow, 119991, Russia; ORCID 0000-0003-4898-4662; ivan.a.novikov@gmail.com

Valery V. Voronov – Prokhorov General Physics Institute of the Russian Academy of Sciences, Moscow, 119991, Russia; ORCID 0000-0001-5029-8560; voronov@lst.gpi.ru

Lubov V. Badyanova – Prokhorov General Physics Institute of the Russian Academy of Sciences, Moscow, 119991, Russia; badyanova.lubov@gmail.com

Sergey V. Kuznetsov – Prokhorov General Physics Institute of the Russian Academy of Sciences, Moscow, 119991, Russia; ORCID 0000-0002-7669-1106; kouznetzovsv@gmail.com

Elena V. Chernova – Prokhorov General Physics Institute of the Russian Academy of Sciences, Moscow, 119991, Russia; ORCID 0000-0001-7401-5019; e-chernova@yandex.ru

Conflict of interest: the authors declare no conflict of interest.